



# 1 A simple model of the turnover of organic carbon in a soil 2 profile: model test, parameter identification and sensitivity

3 Elsa Coucheney<sup>1</sup>, Anke M. Herrmann<sup>1</sup>, Nicholas Jarvis<sup>1</sup>

4 <sup>1</sup>Department of Soil and Environment, Swedish University of Agricultural Sciences, Lennart Hjelm's väg 9, 756  
5 51 Uppsala, Sweden

6 *Correspondence to:* Elsa Coucheney (elsa.coucheney@slu.se)

7 **Abstract.** Simulation models are potentially useful tools to test our understanding of the processes involved in  
8 the turnover of soil organic carbon (SOC) and to evaluate the role of management practices in maintaining stocks  
9 of SOC. We describe here a simple model of SOC turnover at the soil profile scale that accounts for two key  
10 processes determining SOC persistence (i.e. microbial energy limitation and physical protection due to soil  
11 aggregation). We tested the model and evaluated the identifiability of key parameters using topsoil SOC contents  
12 measured in three treatments with contrasting organic matter inputs (i.e. fallow, mineral fertilized and cropped,  
13 with and without straw addition) in a long-term field trial. The estimated total input of organic matter (OM) in  
14 the treatment with straw added was roughly three times that of the treatment without straw addition, but only  
15 12% of the additional OM input remained in the soil after 54 years. By taking microbial energy limitation and  
16 enhanced physical protection of root residues into account, the model could explain the differences in C  
17 persistence among the three treatments, whilst also accurately matching the time-courses of SOC contents using  
18 the same set of model parameters. Models that do not explicitly consider microbial energy limitation and  
19 physical protection would need to adjust their parameter values (either decomposition rate constants or the  
20 retention coefficient) to match this data.

21 We also performed a sensitivity analysis to identify the most influential parameters in the model determining soil  
22 profile stocks of OM at steady-state. Input distributions for soil and crop parameters in the model were defined for  
23 the agricultural production area of PO4 (east-central Sweden), which includes Uppsala. The resulting model  
24 predictions compared well with aggregated soil survey data for the PO4 region. This analysis showed that model  
25 parameters affecting SOC decomposition rates, including the rate constant for microbial-processed SOC and the  
26 parameters regulating physical protection and microbial energy limitation, are more sensitive than parameters  
27 determining OM inputs. Thus, the development of pedotransfer approaches to estimate SOC decomposition rates  
28 from soil properties would help to support predictive applications of the model at larger spatial scales.

## 29 1 Introduction

30 Adopting soil and crop management practices that increase stocks of soil organic carbon (SOC) is one promising  
31 way to mitigate climate change, whilst simultaneously improving soil health (Paustian et al., 2016; Baveye et al.,  
32 2020). In conjunction with long-term field experiments, simulation models are useful tools for testing our  
33 understanding of the processes involved in the turnover of SOC and for evaluating the potential of management  
34 practices to enhance SOC sequestration. Most model applications to date have focused on the topsoil, which is  
35 clearly of major importance with respect to the effects of soil management on SOC and soil health. However,  
36 subsoils contain a large proportion of the total stock of SOC (Batjes, 1996; Jobbágy and Jackson, 2000; Poeplau  
37 et al., 2020) and residence times are also much longer (Rumpel and Kögel-Knabner, 2011; Sierra et al., 2024;



38 Button et al., 2024). This may indicate a significant potential for long-term C sequestration of root-derived OM in  
39 subsoils, which could be of substantial benefit in mitigating climate change.

40 Several detailed mechanistic models have recently been developed that describe a wide range of processes  
41 affecting C stocks at the scale of the entire soil profile, including soil water flow, transport of dissolved organic  
42 carbon by advection-diffusion and bioturbation, as well as descriptions of SOC decomposition explicitly  
43 accounting for microbial processes (e.g. Izaurre et al., 2006; Braakhekke et al., 2011; Riley et al., 2014; Ahrens  
44 et al., 2015; Camino-Serrano et al., 2018; Hicks Pries et al., 2018; Keyvanshokouhi et al., 2019; Yu et al., 2020).  
45 Such mechanistic models are useful tools for improving process understanding (Smith et al., 2018; Derrien et al.,  
46 2023), but parameter uncertainty and the ever-present likelihood of equifinality means that predictive model  
47 applications may be problematic (Braakhekke et al., 2013). Simpler empirical (phenomenological) models of SOC  
48 turnover and storage may have an advantage in this respect because they require fewer parameters (Derrien et al.,  
49 2023).

50 Although simple models are in principle well suited to policy and management applications, their validation status  
51 is generally poor: many have been extensively calibrated against field observations, but their reliability in  
52 extrapolation (i.e. prediction of independent data) has not yet been convincingly demonstrated (Garsia et al., 2023;  
53 Le Noë et al., 2023). Furthermore, these models have almost exclusively been tested using measurements in  
54 topsoil. This is because data for subsoils is rarely available and the turnover of organic C in subsoil is very slow,  
55 so datasets will rarely be long enough to detect any changes. One possibility to test predictions for subsoils is to  
56 make use of  $^{14}\text{C}$  concentrations as a measure of SOC age (e.g. Braakhekke et al., 2014; Ahrens et al., 2015; Sierra  
57 et al., 2018) or concentrations of natural stable isotopes of C (Balesdent and Mariotti, 1987), their ratio  $^{12}\text{C}/^{13}\text{C}$  in  
58 C3-C4 vegetation chronosequences (Schiedung et al., 2017) or labelled material (Sanaullah et al., 2011). If such  
59 data is missing, an alternative approach to model validation is to compare model predictions against spatial (soil  
60 survey) datasets either at catchment, regional or national scales. This has often been done for the topsoil (e.g.  
61 Sleutel, et al., 2006; Yagasaki and Shirato, 2014), but to our knowledge there are no examples of this approach in  
62 the published literature dealing with total stocks of organic C in the profile.

63 Ideally, a model that is intended for predictive applications should combine the advantages of simplicity with  
64 descriptions that adequately capture or mimic the most important processes determining SOC stocks for the  
65 temporal and spatial scales of interest (Campbell and Paustian, 2015). In this respect, the evidence suggests that  
66 turnover of SOC is affected mostly by bioavailability (i.e. soil properties controlling adsorption; Mathieu et al.,  
67 2015), physical protection (e.g. Salomé et al., 2010) and the amount of SOC as it provides energy for microbial  
68 biomass growth, maintenance and activity (e.g. Fontaine et al., 2007; Don et al., 2013; Guenet et al., 2013). In this  
69 study, we describe a simple model that is specifically designed to mimic these key processes at the scale of a soil  
70 profile. The model structure is based on the ICBM model described by Andrén and Kätterer (1997), which contains  
71 two C pools (young particulate and old microbial processed SOC). This simple model based on first-order kinetics  
72 was further developed by Meurer et al. (2020) to account for the interactions of soil organic matter (SOM) with  
73 soil physical properties to enable simulation of physical protection due to soil aggregation. More recently,  
74 Coucheney et al. (2024) further developed the model to account for the effects of SOC stocks on decomposition  
75 rates due to microbial energy limitation (i.e. positive and negative priming) following an approach originally  
76 proposed by Wutzler and Reichstein (2013). Compared with the original ICBM model (Andrén and Kätterer,



77 1997), this new model only requires two additional parameters, one to account for physical protection and one for  
78 microbial energy limitation. It is therefore still relatively simple, neglecting several potentially important processes  
79 affecting SOC stocks in the soil profile, particularly transport processes such as the advection and diffusion of  
80 dissolved organic C as well as bioturbation. However, using a more complex process-oriented model, Sierra et al.  
81 (2024) recently concluded that these transport processes are generally only of limited importance for subsoil SOC  
82 stocks, which are instead largely determined by the balance between root-derived inputs and decomposition rates.

83 Coucheney et al (2024) introduced this simple model of SOC turnover into the new soil-crop model USSF (Jarvis  
84 et al., 2024) and used it to evaluate the potential of winter wheat ideotypes with improved root system  
85 characteristics to enhance SOC stocks in a structured clay soil in Uppsala. In doing so, Coucheney et al. (2024)  
86 parameterized the SOC model from literature information, as the available site data was thought to be insufficient  
87 to unequivocally identify the model parameters. In this paper, we describe the SOC model and present a test of  
88 model predictions and parameter identifiability using organic C concentrations measured in the topsoil of three  
89 treatments with strongly contrasting OM inputs in a long-term field experiment in Uppsala. We also perform a  
90 Monte Carlo sensitivity analysis to identify the most influential parameters in the model determining estimates of  
91 total stocks of SOC in the soil profile at steady-state. Input distributions for soil and crop parameters were defined  
92 for the agricultural production area (PO4) in east-central Sweden that encompasses Uppsala. Geo-referenced data  
93 that would enable a spatially explicit test of the model for this region was not available. Instead, aggregated  
94 regional-scale soil survey data was used as a qualitative “reality-check”, assuming that profiles of SOC are  
95 approximately at steady-state.

## 96 **2 Materials and Methods**

97 In the following, we first describe a new parsimonious model of OM turnover applicable to a single topsoil layer,  
98 which we test using data from three contrasting cropping and fertilization treatments in the Ultuna Long-Term Soil  
99 Organic Matter Experiment. We then derive a steady-state solution of the model and also show how it can be  
100 extended to describe OM storage and turnover in a complete soil profile. Finally, these profile-scale steady-state  
101 solutions are used to support a regional-scale sensitivity analysis and reality-check.

### 102 **2.1 Model description**

#### 103 **2.1.1 SOM turnover and storage in a single soil layer**

104 A dual-porosity model describing the two-way interactions between soil physical properties and SOM stocks and  
105 turnover was described by Meurer et al. (2020). In this model, SOM contents influence the total porosity and its  
106 partitioning between two pore regions in the soil (i.e. mesopores and micropores) using a simple model that  
107 describes how SOM affects aggregation. In turn, the pore size distribution determines the partitioning of root-  
108 derived inputs of OM between the two pore regions and also regulates decomposition rates as a consequence of  
109 the physical protection of OM in microporous regions of the soil. Coucheney et al. (2024) introduced a description  
110 of the effects of microbial energy limitation according to the “*LimUptake*” variant of the model suite described by  
111 Wutzler and Reichstein (2013) into the SOM model described by Meurer et al. (2020). They also simplified the  
112 description of the transfer of SOM between the two pore regions by tillage, making the assumption that there is  
113 always a net transfer of SOM from micropore to mesopore regions. This should give more realistic simulations of  
114 the effects of tillage on SOM and also has the added benefit of allowing a straightforward solution of the model  
115 for steady-state conditions.



116 The model tracks four pools of SOM, two pools of young OM ( $M_{Y(mic)}$  and  $M_{Y(mes)}$ ) and two pools of older  
 117 microbial-processed SOM ( $M_{O(mic)}$  and  $M_{O(mes)}$ ). For both types, one part is stored in microporous regions of the  
 118 soil (subscript “mic”) where it is partially protected from decomposition, while the remainder is stored in regions  
 119 of the soil in contact with larger mesopores (subscript “mes”), which facilitates faster decomposition. Changes in  
 120 the mass of SOM in the four pools ( $\text{kg m}^{-2}$ ) in a layer are given by:

$$121 \quad \frac{dM_{Y(mes)}}{dt} = I_a + I_r(1 - f_{r,mic}) - k_Y k_{u(mes)} M_{Y(mes)} + k_{till} M_{Y(mic)} \quad (1)$$

$$122 \quad \frac{dM_{O(mes)}}{dt} = (\varepsilon k_Y k_{u(mes)} M_{Y(mes)}) - ((1 - \varepsilon) k_O k_{u(mes)} M_{O(mes)}) + k_{till} M_{O(mic)} \quad (2)$$

$$123 \quad \frac{dM_{Y(mic)}}{dt} = I_r f_{r,mic} - k_Y k_{u(mic)} F_p M_{Y(mic)} - k_{till} M_{Y(mic)} \quad (3)$$

$$124 \quad \frac{dM_{O(mic)}}{dt} = (\varepsilon k_Y k_{u(mic)} F_p M_{Y(mic)}) - ((1 - \varepsilon) k_O k_{u(mic)} F_p M_{O(mic)}) - k_{till} M_{O(mic)} \quad (4)$$

125 where  $I_a$  and  $I_r$  ( $\text{kg m}^{-2} \text{yr}^{-1}$ ) are the supply of OM from above-ground residues and roots respectively,  $f_{r,mic}$  (-) is  
 126 the proportion of the root-derived OM added to the micropore region,  $\varepsilon$  (-) is the SOM retention coefficient,  $k_Y$  and  
 127  $k_O$  ( $\text{yr}^{-1}$ ) are reference rate constants for the decomposition of young and old SOM,  $k_{till}$  ( $\text{yr}^{-1}$ ) is rate constant  
 128 regulating the transfer of SOM between pore regions by tillage,  $F_p$  (-) is a factor varying from zero to unity that  
 129 reduces OM decomposition rates in the micropore region to account for physical protection and  $k_{u(mes)}$  and  $k_{u(mic)}$   
 130 (-) are microbial energy limitation factors given by the simple model described by Wutzler and Reichstein (2013):

$$131 \quad k_{u(mes)} = \max \left\{ 0; \left( 1 - \frac{A_a}{\varepsilon \left( k_Y \left( \frac{M_{Y(mes)}}{\Delta z} \right) + k_O \left( \frac{M_{O(mes)}}{\Delta z} \right) \right)} \right) \right\} \quad (5)$$

$$132 \quad k_{u(mic)} = \max \left\{ 0; \left( 1 - \frac{A_a}{\varepsilon F_p \left( k_Y \left( \frac{M_{Y(mic)}}{\Delta z} \right) + k_O \left( \frac{M_{O(mic)}}{\Delta z} \right) \right)} \right) \right\} \quad (6)$$

133 where  $A_a$  ( $\text{kg m}^{-3} \text{yr}^{-1}$ ) is a composite microbial parameter that represents a minimum C uptake flux that can support  
 134 an active microbial biomass and  $\Delta z$  is the layer thickness (m).

135 Soil bulk density,  $\gamma_b$  ( $\text{kg m}^{-3}$ ) and OM content  $f_{som}$  ( $\text{kg kg}^{-1}$ ) are calculated from the stocks of OM as inter-linked  
 136 variables (Meurer et al., 2020):

$$137 \quad \gamma_b = \frac{M_{tot} + (\Delta z_{min} \gamma_m (1 - \phi_{min}))}{\Delta z} \quad (7)$$

$$138 \quad f_{som} = \frac{M_{tot}}{\Delta z \gamma_b} \quad (8)$$

139 where  $M_{tot}$  ( $\text{kg m}^{-2}$ ) is the total OM stock ( $= M_{Y(mes)} + M_{O(mes)} + M_{Y(mic)} + M_{O(mic)}$ ),  $\gamma_m$  ( $\text{kg m}^{-3}$ ) is the density of mineral  
 140 matter in soil and  $\phi_{min}$  is the textural porosity in soil ( $\text{m}^3 \text{m}^{-3}$ ). The layer thickness in equations 5 to 8 varies due to  
 141 soil aggregation (Meurer et al., 2020):

$$142 \quad \Delta z = \Delta z_{min} + \left\{ (1 + f_{agg}) \left( \frac{M_{tot}}{\gamma_o} \right) \right\} \quad (9)$$

143 where  $f_{agg}$  ( $\text{m}^3 \text{m}^{-3}$ ) is the aggregation factor,  $\gamma_o$  ( $\text{kg m}^{-3}$ ) is the density of SOM and  $\Delta z_{min}$  (m) is the minimum layer  
 144 thickness in a soil without SOM and aggregation porosity.



145 Meurer et al. (2020) equated  $f_{r,mic}$  in equations 1 and 3 with the micropore fraction of the soil pore space, which  
 146 varied with changes in OM stocks in each pore region. Here, in order to derive a solution for OM stocks at steady-  
 147 state (see “Steady-state solution for SOM stocks”), the fraction of the root-derived OM added to the micropore  
 148 region ( $f_{r,mic}$  in equations 1 and 3) is assumed to be a constant and is calculated from a micropore fraction of the  
 149 pore space  $f_{mic}$  (-) estimated from the soil clay content, weighted by a dimensionless constant  $w$  ( $0 \leq w \leq 1$ ) to  
 150 account for the effects of soil strength on the distribution of roots between the two pore regions. Using a power  
 151 law function for the pore size distribution gives:

$$152 \quad f_{r,mic} = w f_{mic} = w \left( \frac{\psi_{ae}}{\psi_{mic}} \right)^\lambda \quad (10)$$

153 where  $\psi_{ae}$  and  $\psi_{mic}$  are the air-entry pressure head (m) and the pressure head (m) equivalent to the largest micropore  
 154 in the soil respectively and  $\lambda$  (-) is the pore size distribution index (Brooks and Corey, 1964), which is here  
 155 estimated from soil clay content  $f_{clay}$  (kg kg<sup>-1</sup>) using the pedotransfer functions for field capacity  $\theta_{fc}$  and wilting  
 156 point  $\theta_w$  (m<sup>3</sup> m<sup>-3</sup>) derived from a database of water retention curves for Swedish agricultural soils by Kätterer et  
 157 al. (2006):

$$158 \quad \lambda = \frac{\log\left(\frac{\theta_w}{\theta_{fc}}\right)}{\log\left(\frac{0.5}{150}\right)} \quad (11)$$

$$159 \quad \theta_{fc} = 0.27 + 0.325 f_{clay} \quad (12)$$

$$160 \quad \theta_w = 0.004 + 0.5 f_{clay} \quad (13)$$

161 Thus, in this simpler version of the model described by Meurer et al. (2020), changes in SOM contents affect the  
 162 porosity and bulk density but not the pore size distribution.

### 163 2.1.2 Steady-state solution for SOM stocks

164 From equations 1 to 4, steady-state SOM stocks in the four pools are given as:

$$165 \quad M_{Y(mic)} = \left( \frac{I_r f_{r,mic}}{\{k_Y F_p k_{u,mic}\} + k_{till}} \right) \quad (14)$$

$$166 \quad M_{Y(mes)} = \left( \frac{I_a + I_r (1 - f_{r,mic}) + \{k_{till} M_{Y(mic)}\}}{k_Y k_{u,mes}} \right) \quad (15)$$

$$167 \quad M_{O(mic)} = \left( \frac{\varepsilon k_Y k_{u,mic} F_p M_{Y(mic)}}{\{(1-\varepsilon)k_O F_p k_{u,mic}\} + k_{till}} \right) \quad (16)$$

$$168 \quad M_{O(mes)} = \left( \frac{\{\varepsilon k_Y k_{u,mes} M_{Y(mes)}\} + k_{till} M_{O(mic)}}{(1-\varepsilon)k_O k_{u,mes}} \right) \quad (17)$$

169 Equations 14 to 17 show that the steady-state stocks depend on  $k_u$ , while  $k_u$ , in turn, depends on the stocks  
 170 (equations 5 and 6). An iterative procedure is first used to derive a value of  $k_{u(mic)}$  at steady-state that simultaneously  
 171 satisfies equations 6, 14 and 16. The steady-state stocks in the mesopore region (equations 15 and 17) depend on  
 172 the value of  $k_{u,mes}$  at steady-state.

173



174 This can now be calculated directly by substituting equations 15 and 17 into equation 5:

$$175 \quad k_{u,mes} = \frac{1}{1 + \left\{ \frac{A_a \Delta z}{\varepsilon \left( i^* + \left( \frac{\varepsilon i^* + k_{till} M_{O(mic)}}{1 - \varepsilon} \right) \right)} \right\}} \quad (18)$$

176 where  $i^*$  is the input of OM to the mesopore region given by:

$$177 \quad i^* = I_a + I_r(1 - f_{r,mic}) + k_{till} M_{Y(mic)} \quad (19)$$

### 178 2.1.3 Application of the model to a soil profile

179 The model can be applied to a soil profile consisting of two or more soil horizons by expressing  $k_{till}$ ,  $I_a$ ,  $I_r$ , and  $w$   
 180 as a function of soil depth, keeping all the other parameters constant. Tillage is here assumed to affect SOM  
 181 turnover only in the uppermost horizon, with  $k_{till}$  set to zero for all other horizons. Above-ground crop residues  $I_a$   
 182 are given by:

$$183 \quad I_a = Y \left( \frac{1}{HI} - 1 \right) f_{inc} \quad (20)$$

184 where  $Y$  is the yield ( $\text{kg m}^{-2}$ ),  $HI$  (-) is the harvest index (the ratio of yield to total above-ground biomass) and  $f_{inc}$   
 185 is the proportion of the above-ground residues incorporated into soil. The partitioning of  $I_a$  among the soil horizons  
 186 can be defined by the user, but should reflect tillage systems and depths of cultivation. The total input of root-  
 187 derived OM,  $I_r$  is given by:

$$188 \quad I_{r(tot)} = \frac{Y f_{bg}}{HI(1 - f_{bg})} \quad (21)$$

189 where  $f_{bg}$  is the proportion of net primary production that is allocated below-ground, including both root growth  
 190 and exudates. Root-derived OM is added to the soil horizons in the profile according to a two-parameter logistic  
 191 function, which represents the distribution of roots with depth in the soil (e.g. Schenk and Jackson, 2002; Fan et  
 192 al., 2016):

$$193 \quad P = \frac{1}{1 + \left( \frac{z}{D_{50}} \right)^c} \quad (22)$$

194 where  $P$  is the fraction of the total root biomass found above a depth  $z$ , representing the lower boundary of the  
 195 horizon in question,  $c$  is a root distribution parameter and  $D_{50}$  is the depth above which 50% of the root biomass  
 196 is recovered, which is given by:

$$197 \quad D_{50} = \frac{D_{95}}{\left( \frac{1}{0.95} - 1 \right)^{\frac{1}{c}}} \quad (23)$$

198 where  $D_{95}$  is the depth (m) above which 95% of the total root biomass is recovered. With this function, a small  
 199 fraction of the root biomass is found below the depth of the soil profile. This additional fraction of the root biomass  
 200 is added to the upper two horizons in equal amounts.

201 Finally, the weighting function to account for the effects of soil strength on the distribution of roots between the  
 202 two pore regions is given by:

$$203 \quad w = EXP(-w_s(z - z_1)) \quad (24)$$



204 where the constant  $w_s$  ( $\text{m}^{-1}$ ) reflects the effects of increasing soil strength with depth on the distribution of roots  
205 between soil micropore and mesopore regions and  $z_l$  is the depth to the lower boundary of the uppermost soil  
206 horizon. It can be seen from equation 24 that  $w = 1$  for the uppermost horizon, so that the root-derived OM in this  
207 layer is partitioned between the pore regions directly proportional to their estimated respective partial volumes.

## 208 2.2 Model applications

### 209 2.2.1 Long-term transient simulations of SOC under contrasting cropping and fertilization

210 We performed a test of the model described by equations 1 to 13 using data from the Ultuna Long-Term Soil  
211 Organic Matter Experiment located at Uppsala, east-central Sweden (59.8°N, 17.7°E, Fig. 1). The mean annual  
212 temperature at Ultuna is 7°C and the mean annual precipitation is 570 mm. The texture in the uppermost 20 cm of  
213 soil is clay loam (37% clay, 41% silt and 22% sand). In this study, we make use of SOC contents measured in the  
214 topsoil (0-20 cm depth) from the start of the trial in 1956 until 2010 in three treatments with contrasting inputs of  
215 organic matter: an uncropped fallow treatment (“Fallow”) and two cropped treatments (“N fertilized” and “N  
216 fertilized + straw”), both of which are supplied with  $\text{Ca}(\text{NO}_3)_2$  every year at the time of sowing at a rate of 80 kg  
217  $\text{N ha}^{-1} \text{ year}^{-1}$ . Most (ca. 95%) of the above-ground crop residues are removed at harvest in autumn and straw is  
218 applied biennially to the treatment “N fertilized + straw” after harvest at an equivalent annual rate of 4.2  $\text{t ha}^{-1}$ .  
219 Maize has been grown on the cropped plots since 2000. Before 2000, the crop rotation included barley, oats, beets  
220 (prior to 1967) and rape. All the plots are dug by hand after harvest each year to a depth of 20 cm. We refer readers  
221 to Persson and Kirchmann (1994) and Kätterer et al. (2011) for more details of the design of the field experiment.



222  
223 **Figure 1. Map showing the location of the Ultuna Long-term Soil Organic Matter Experiment (Uppsala,**  
224 **Sweden) and the extent of the production area PO4 (Drawn by Anna Lindahl, SLU from Esri, TomTom,**  
225 **Garmin, FAO, NOAA, USGS)**



226 Inputs of OM from above- and below-ground crop residues were estimated following Kätterer et al. (2011), who  
 227 made use of the allocation functions dependent on crop yields derived by Bolinder et al. (2009), together with a  
 228 Michaelis-Menten function to estimate the proportion of the root-derived OM that was presumed to have been  
 229 input to the topsoil (0-20 cm). Here, we simplified this method by using average OM inputs in each treatment for  
 230 the experimental period (1956-2010) based on annual values calculated for the different crops in the rotation.

231 The model was simultaneously calibrated to the measurements from the three treatments using the Generalized  
 232 Likelihood Uncertainty Estimation (GLUE) method (Beven, 2006; Beven and Binley 2014; Juston et al., 2010).  
 233 Inspection of the model equations led us to expect to encounter significant equifinality. All but six of the model  
 234 parameters were therefore set to fixed values (Table 1). These included the soil physical properties, since an  
 235 analysis of soil structure dynamics was not the main focus of this modelling study, which employs a slightly  
 236 simplified description of the interactions between soil aggregation and SOM. Nevertheless, the final bulk densities  
 237 simulated with the parameterization shown in Table 1 varied between 1.2 and 1.3 g cm<sup>-3</sup> in the three treatments  
 238 (“Fallow” > “N fertilized” > “N fertilized + straw”), which match reasonably well the values reported in Kätterer  
 239 et al. (2011).

240 **Table 1. Model parameters fixed at constant values during the calibration**

Parameter	Symbol	Units	Value
Clay content	$f_{clay}$	kg kg <sup>-1</sup>	0.36
Density of organic matter	$\gamma_o$	kg m <sup>-3</sup>	1200
Density of mineral matter	$\gamma_m$	kg m <sup>-3</sup>	2700
Textural porosity	$\phi_{min}$	m <sup>3</sup> m <sup>-3</sup>	0.5
Aggregation factor	$f_{agg}$	m <sup>3</sup> m <sup>-3</sup>	3
Physical protection factor	$F_p$	-	0.2
Air-entry pressure head	$\psi_{ae}$	m	0.2
Pressure head equivalent to the largest micropore in soil	$\psi_{mic}$	m	6.0
Reference decomposition rate constant for young OM	$k_y$	year <sup>-1</sup>	0.8

241 Table 2 shows the prior uncertainty ranges for the six parameters. The OM supply prior to the start of the  
 242 experiment and the fraction of this OM supplied as straw, were included in the calibration process to help initialize  
 243 the SOM pools during a common 5000-year spin-up period. Four remaining parameters, which were considered  
 244 difficult to identify “a priori” from experimentation, but which were thought to be sensitive and therefore  
 245 potentially identifiable by calibration, were treated as uncertain (Table 2). We ran 12000 simulations using Latin  
 246 Hypercube Sampling to sample uniform distributions between the minimum and maximum values for the six  
 247 uncertain parameters (Table 2).

248 The model efficiency  $EF$  was used as the likelihood function in GLUE:

$$249 \quad EF = 1 - \frac{\sum_{i=1}^n (O_i - P_i)^2}{\sum_{i=1}^n (O_i - \bar{O})^2} \quad (25)$$

250 where  $O$  and  $P$  are observed and predicted values,  $\bar{O}$  is the mean of the observations and  $n$  is the number of  
 251 observations. The maximum value of  $EF$  is one, when predictions and observations are identical, while a negative  
 252 value implies a poor model, since it means that taking the average of the observations would give a better  
 253 prediction. For each simulation, individual model efficiencies were calculated for each treatment and the mean  $EF$   
 254 value for the three treatments was used as a metric to identify acceptable parameters sets.





255 **Table 2. Initial parameter uncertainty ranges for the model calibration to the Ultuna Long-Term Soil**  
256 **Organic Matter Experiment**

Parameter	Symbol	Units	Prior uncertainty bounds
Total OM input during spin-up	$I_a + I_r$	kg m <sup>-2</sup> year <sup>-1</sup>	0.25 – 0.45
Straw fraction of OM input during spin-up	$I_a/(I_a + I_r)$	-	0.65 – 0.85
Rate constant for OM transfer by tillage between pore regions	$k_{till}$	year <sup>-1</sup>	0 – 0.01
Reference decomposition rate constant for old organic matter	$k_o$	year <sup>-1</sup>	0.06 – 0.1
OM retention coefficient	$\varepsilon$	-	0.20 – 0.45
Microbial energy limitation factor	$A_a$	kg m <sup>-3</sup> year <sup>-1</sup>	0.1 – 0.3

257 **2.2.2 Steady-state calculations: sensitivity analysis and reality-check**

258 We performed a Monte Carlo sensitivity and uncertainty analysis to assess the relative importance of 15 model  
259 parameters for predictions of the steady-state stocks of SOM in the soil profile (equations 7 to 24). The analysis  
260 was based, to the extent possible, on data and information available for the Ultuna field site as well as soil survey  
261 and cropping data (e.g. crop yields, soil clay content) for the agricultural production area PO4 in east-central  
262 Sweden (i.e. the region in which Ultuna is located, Fig. 1). Literature information was used to determine parameter  
263 distributions in the absence of data at the local or regional scale (Table 3). We assumed normal distributions when  
264 the data support was considered sufficient, while uniform distributions were used otherwise (Table 3). One  
265 thousand parameter sets were generated from these distributions by random sampling.

266 Calculations were performed for a soil profile 120 cm in depth, divided into four soil horizons (0-20, 20-40, 40-  
267 60 and 60-120 cm). We added 80% of the above-ground residues  $I_a$  (equation 20) to the uppermost horizon in the  
268 soil profile and the remaining 20% to the horizon below. For all 1000 parameter sets, we calculated the SOM stock  
269 in each horizon and in the whole soil profile at steady-state. For each soil horizon, we also calculated the steady-  
270 state bulk density and SOM contents as well as the mean residence time of SOM as the steady-state SOM stock  
271 divided by the input/output flux.

272 We used a multiple linear regression model to characterize variations in the steady-state SOM stocks in the profile  
273 ( $y$ ), such that the normalized coefficients ( $\beta_1, \beta_2 \dots \beta_n$ ) can be used as a metric of sensitivity to variation in the  
274 parameters ( $x_1, x_2 \dots x_n$ ) (Saltelli and Annoni, 2010):

$$275 \quad y = \beta_0 + \beta_1 x_1 + \beta_2 x_2 + \dots + \beta_n x_n \quad (26)$$

276 Aggregated data for SOC contents measured at three depth intervals (0-20, 20-40 and 40-60 cm depth) for soils in  
277 production area PO4 (n = 611, 100 and 100 respectively) were extracted from the national soil and crop inventory  
278 carried out from 2001 to 2007 (Eriksson et al., 2010) and used as a qualitative "reality-check" for the model  
279 calculations. Note that, as a consequence of simulating links to soil physical properties, the model calculates SOM  
280 contents, whereas SOC was measured. In converting from one to the other, we assumed that organic C constituted  
281 50% of the SOM. Likewise, calculated bulk densities at zero to 20 cm and 40 to 60 cm depth were compared with  
282 data available for soil profiles (n = 54) located in the production area PO4 (Klöffel et al., 2024). The model  
283 parameters required to convert calculated SOM stocks to estimates of SOM contents using equations 7 to 9 were  
284 set to the fixed values used in the model calibration (Table 1), with the exception of the textural porosity which



285 was reduced from 0.5 to 0.4, as the latter value was considered to be more representative for most soils (Klöffel et  
 286 al., 2024).

287 **Table 3. Parameter input distributions in the sensitivity analysis**

Group	Parameter and symbols		Units	Distribution	Min./Max or Mean/St. dev	Source
Crop growth and residue inputs	Yield	$Y$	kg m <sup>-2</sup>	Normal	0.5; 0.05	SCB, Statistics Sweden
	Harvest index	$HI$	-	Normal	0.4; 0.05	Site data; Hay (1995)
	Fraction of net primary production allocated below-ground	$f_{bg}$	-	Normal	0.2; 0.025	Bolinder et al. (2007); Kätterer et al. (2011)
	Fraction of above-ground crop residues incorporated	$f_{inc}$	-	Normal	0.65; 0.1	Smerald et al. (2023)
	Root depth	$D_{95}$	m	Uniform	0.8; 1.2	Jackson et al. (1996); Kätterer et al. (2011); Fan et al. (2016)
	Root distribution factor	$c$	-	Uniform	-1.2; -0.9	Fan et al. (2016)
Tillage	Rate constant for OM transfer between pore regions	$k_{ill}$	y <sup>-1</sup>	Uniform	0; 0.006	This study
Organic matter turnover	Reference decomposition rate constant for young organic matter	$k_Y$	y <sup>-1</sup>	Uniform	0.6; 1.0	Andrén and Kätterer (1997)
	Reference decomposition rate constant for old organic matter	$k_O$	y <sup>-1</sup>	Uniform	0.06; 0.1	This study
	OM retention coefficient	$\epsilon$	-	Uniform	0.30; 0.35	This study
	Physical protection factor	$F_p$	-	Uniform	0.1; 0.3	Kravchenko et al. (2015)
	Microbial energy limitation factor	$A_a$	kg m <sup>-3</sup> y <sup>-1</sup>	Uniform	0.1; 0.3	This study
Soil physical properties	Clay content	$f_{clay}$	kg kg <sup>-1</sup>	Normal	0.3; 0.1	Eriksson et al. (2010)
	Factor for soil strength effects on root distribution between pore regions	$w_s$	m <sup>-1</sup>	Uniform	2; 4	
	Pressure head defining the largest micropore	$\psi_{mic}$	m	Uniform	-30; -6	Killham et al. (1993); Strong et al. (2004); Ruamps et al. (2011)

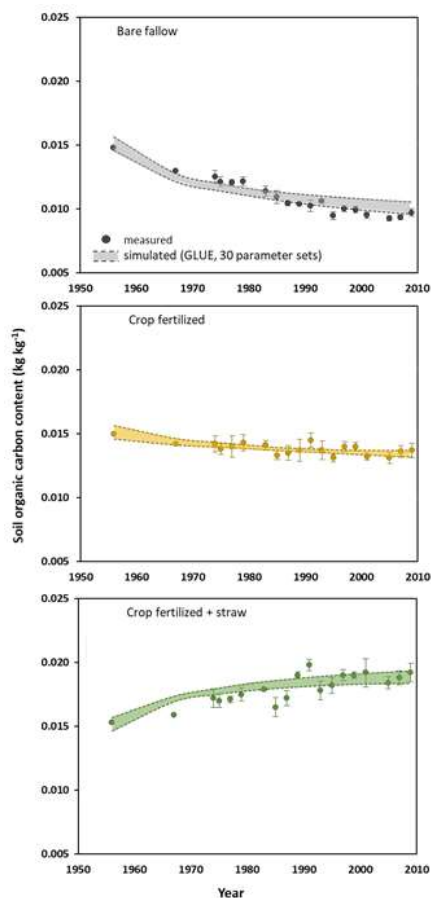


## 288 3 Results and Discussion

### 289 3.1 Long-term transient simulations

290 Figure 2 shows that the model could be calibrated to match simultaneously the changes in SOC contents measured  
291 in the three treatments at the Ultuna Long-Term Soil Organic Matter Experiment during the 50 year period, with  
292 the spread of the simulations from the 30 best parameter sets approximately matching the observed variation in  
293 SOC among the four replicate plots. Table 4 shows simulated SOM balances for the three treatments. The total  
294 input of crop residues in the “N fertilized + straw” treatment is roughly three times that of the “N-fertilized”  
295 treatment without straw addition. The calculated inputs of OM derived from roots were similar (Table 4), so that  
296 larger inputs of straw accounted for almost all of the difference in OM inputs between these two treatments.  
297 However, according to the simulations, almost 88% of the additional OM input in the “N fertilized + straw”  
298 treatment was lost as a consequence of enhanced mineralization, with only 12% remaining in the soil. While above-  
299 ground crop residues are thought to be less persistent in soil than root-derived residues, the relative importance of  
300 several potential underlying mechanisms that could explain this finding is still unclear (e.g. Rasse et al., 2005;  
301 Kätterer et al., 2011). It can be noted here that the model does not consider any differences in the quality of root-  
302 and straw-derived OM. Instead, the model suggests that the comparatively small difference in OM stocks at the  
303 end of the experiment in the two treatments in relation to the large difference in OM inputs is a result of two  
304 processes: firstly, straw incorporated in the “N fertilized + straw” treatment is solely added to the mesopore region,  
305 which does not afford any physical protection. In contrast, a certain proportion,  $f_{mic}$ , of root-derived OM is added  
306 to the physically-protected micropore region. Secondly, mineralization rates in the “N-fertilized” treatment without  
307 straw addition are reduced by microbial energy limitation as a consequence of an overall decrease in OM stocks  
308 due to the export of residues. Taking both these processes into account (physical protection and microbial energy  
309 limitation; see equations 1 to 6) enabled the model to reproduce the time-courses of SOC contents in the two  
310 treatments with identical parameterizations.

311 Figure 3 shows that only one of the parameters included in the calibration procedure (the OM retention coefficient,  
312  $\epsilon$ ) was well constrained by the data, with acceptable values lying within a narrow range (ca. 0.30 to 0.35). In  
313 contrast, for the other five parameters, simulations with large model efficiencies could be found across almost the  
314 entire prior uncertainty ranges (Fig. 3). An inspection of the mathematical structure of the model suggests that  
315 such a high degree of equifinality should be expected, as many of the key parameters should be strongly correlated  
316 (Coucheney et al., 2024). For the 30 best parameter sets, Figure 4 demonstrates that this is indeed the case for the  
317 four parameters regulating decomposition rates in the model ( $\epsilon$ ,  $k_o$ ,  $A_a$  and  $k_{fill}$ ). These strong correlations of  $k_o$ ,  $A_a$   
318 and  $k_{fill}$  with  $\epsilon$  mean that, in practice, all four parameters are well constrained by the calibration. The acceptable  
319 ranges for these four parameters shown in Figure 4 were utilized in the sensitivity analysis (Table 3).

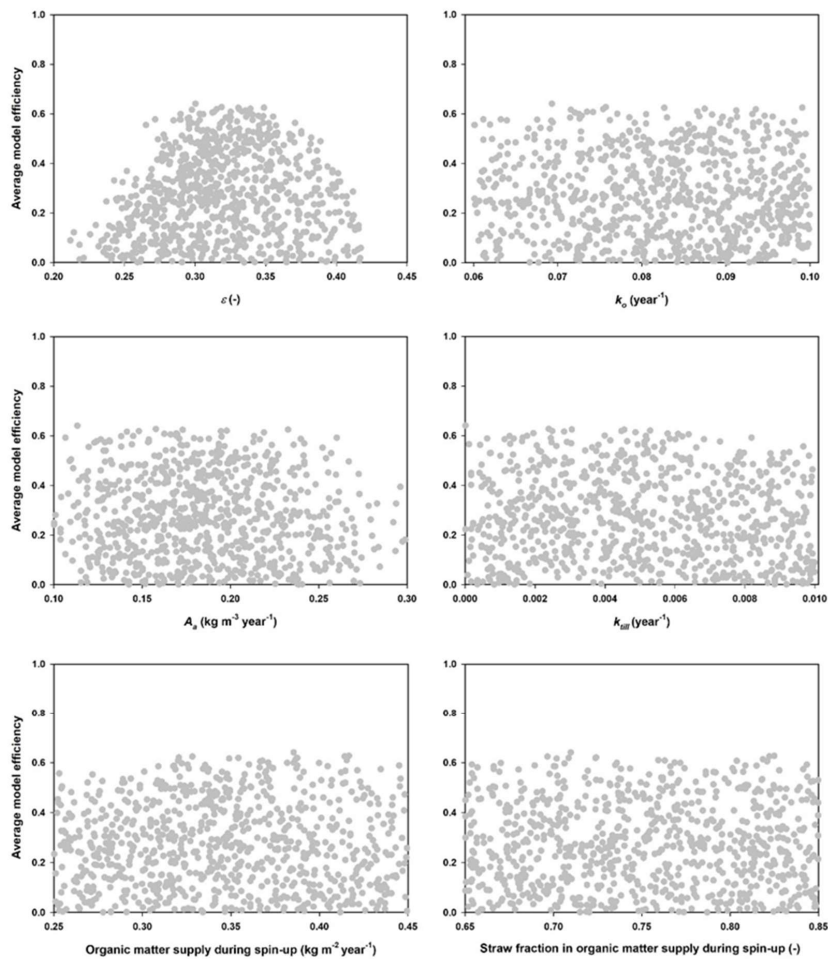


320  
 321 **Figure 2. Comparisons of measured SOC contents (symbols are the means of four replicates and the bars**  
 322 **are standard deviations) with the 30 best simulations from the GLUE analysis (the dashed lines indicate**  
 323 **ranges)**

324 **Table 4. Simulated mass balances ( $\text{kg m}^{-2}$ ) for SOM for the 55-year experimental period (1956 to 2010) at**  
 325 **the Ultuna Long-Term Soil Organic Matter Experiment. Values shown for mineralization are the means**  
 326 **and standard deviations (in brackets) for the 30 best simulations. Values for change of stocks in brackets**  
 327 **are the percentage changes in relation to the original stock of SOM.**

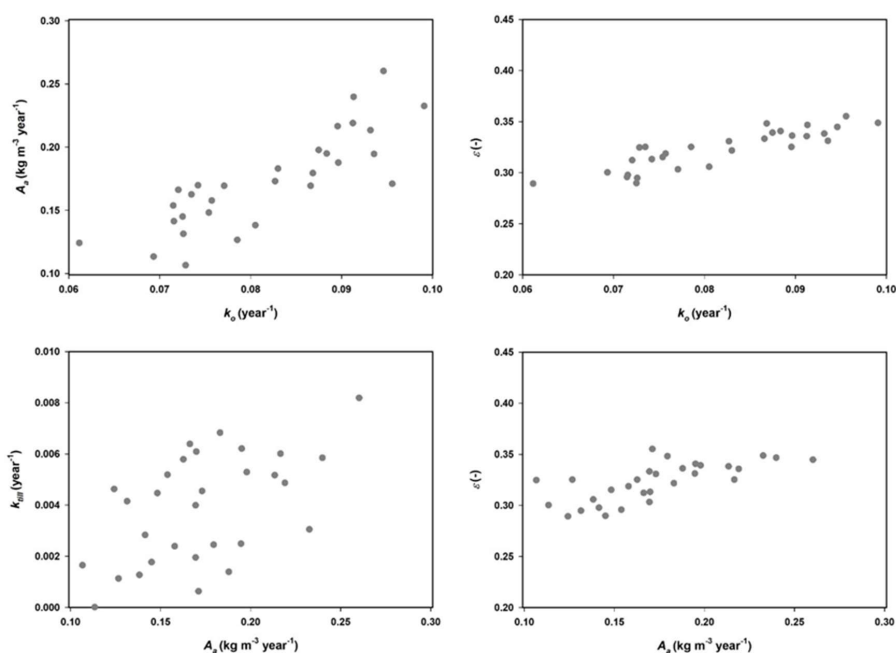
Component	Treatment		
	Fallow	N fertilized	N fertilized + straw
Inputs:			
<sup>1</sup> Estimated below-ground residues	0.44	9.85	10.67
Above-ground residues	0	1.82	22.94
Total crop residue input	0.44	11.67	33.61
Mineralization in soil	3.01 (0.18)	12.53 (0.16)	31.75 (0.20)
Change of SOM stock	-2.57 (-35.1%)	-0.86 (-11.7%)	1.86 (25.4%)

328 <sup>1</sup> estimated using the algorithms presented by Bolinder et al. (2007) and Kätterer et al. (2011)



329

330 **Figure 3. Mean model efficiencies plotted against the values for the six parameters in the GLUE analysis**  
331 **(only simulations with model efficiencies larger than zero are shown in the plots).**



332

333

**Figure 4. Inter-relationships between four model parameters regulating organic matter decomposition in the model for the 30 best parameter sets.**

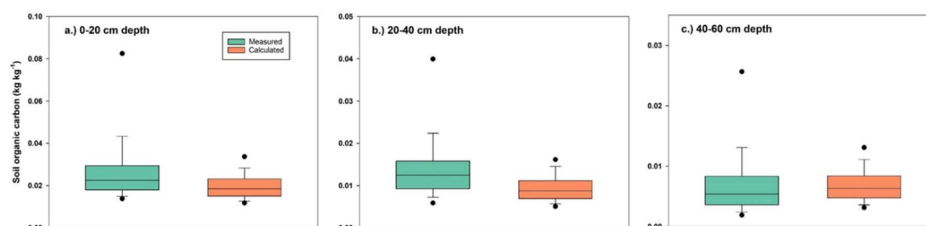
334

### 335 3.2 Steady-state calculations

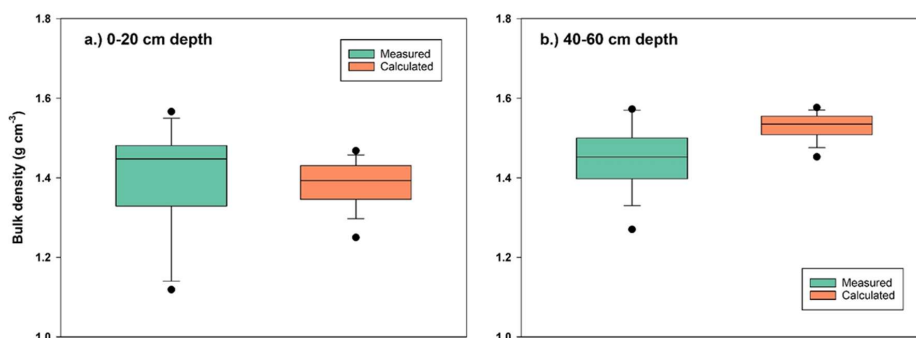
336

A qualitative comparison with soil survey data for agricultural land in east-central Sweden (production area PO4) suggests that despite its simplicity the model gives reasonably realistic predictions of steady-state SOC and bulk density in the soil profile (Fig. 5 and Fig.6). As a further “reality check”, Figure 7 shows distributions of the mean residence times of SOM calculated for the four horizons in the soil profile. Median values (ca. 20 years) and distributions of residence times estimated for the topsoil are similar to those estimated by Poeplau et al. (2021) for German agricultural soils, and they also lie well within the ranges estimated for boreal-temperature climates in the global analysis presented by Chen et al. (2020). This gives us confidence that the results of the sensitivity analysis presented in the following should be reasonably well grounded in reality. As also shown by Coucheney et al. (2024), the model simulates much longer mean residence times in the subsoil horizons, due to microbial energy limitation and physical protection, with median values of ca. 300 years (Figure 7).

345



346  
347 **Figure 5. Comparison of the distributions of SOC contents measured at three depths for soil profiles located**  
348 **in east-central Sweden (production area PO4; Eriksson et al., 2010) with distributions calculated in the**  
349 **model sensitivity analysis. Horizontal lines show median values, the box defines the inter-quartile range,**  
350 **error bars define 10<sup>th</sup> and 90<sup>th</sup> percentiles and solid symbols indicate 5<sup>th</sup> and 95<sup>th</sup> percentiles. Note the**  
351 **differences in the y-axis scales.**

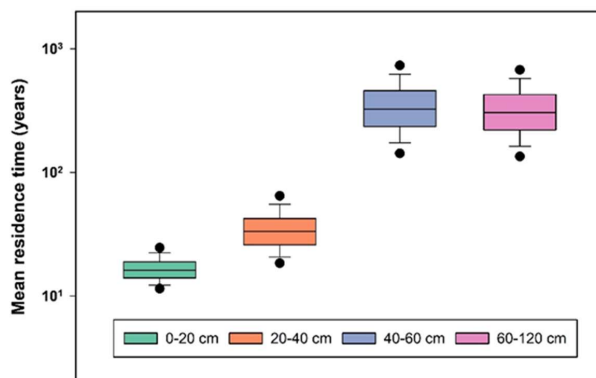


352  
353 **Figure 6. Comparison of the distributions of soil bulk density measured at two depths in soil profiles located**  
354 **in east-central Sweden (production area PO4) with the distributions calculated in the model sensitivity**  
355 **analysis. Horizontal lines show median values, the box defines the inter-quartile range, error bars define**  
356 **10<sup>th</sup> and 90<sup>th</sup> percentiles and solid symbols indicate 5<sup>th</sup> and 95<sup>th</sup> percentiles.**

357 Table 5 shows that the most sensitive parameters in the model are those determining decomposition rates of SOM,  
358 especially the rate constant for microbial-processed OM,  $k_o$ , the parameter regulating microbial energy limitation,  
359  $A_a$ , and the parameter regulating the degree of physical protection of OM stored in micropores,  $F_p$ . The soil clay  
360 content, which strongly affects the extent to which physical protection is expressed in soils of contrasting texture,  
361 is also a relatively sensitive model parameter (Table 5). Not surprisingly, along with the OM retention coefficient,  
362  $\epsilon$ , the two parameters determining total OM inputs (i.e. crop yields and harvest index) also exert a strong control  
363 on SOM stocks in the soil profile (Table 5). The results of the sensitivity analysis also illustrate the importance of  
364 below-ground production for soil profile C stocks calculated by the model (parameter  $f_{bg}$ , fraction of NPP allocated  
365 below-ground; Table 5), reflecting the assumptions in the model concerning the greater persistence of root-derived  
366 OM discussed earlier. An increase of 25% in the fraction of net primary production allocated to roots,  $f_{bg}$ , increases  
367 steady-state SOM stocks by ca. 8%. Transient simulations run with the USSF model for winter wheat grown on  
368 Ultuna clay soil presented by Coucheny et al. (2024) illustrate what might be achievable in a 30-year time  
369 perspective in the context of climate change mitigation: for the same 25% increase in below-ground C allocation,



370 the USSF model simulated increases in C stocks of ca. 1.4%. In contrast to below-ground production, the  
371 sensitivity analysis suggests that root depth and distribution would have little impact on soil profile stocks of OM  
372 (Table 5). However, in comparison with soil-crop models such as USSF, the limitations of the simpler model  
373 described here should be borne in mind, in particular the lack of any feedback between root system development  
374 and crop growth, and thus residue production. In reality, root depth and distribution may play a larger role for soil  
375 C stocks. Thus, the transient simulations performed with the full USSF soil-crop model for winter wheat on Ultuna  
376 clay soil by Coucheney et al. (2024) suggested that deeper rooting would increase water uptake and crop growth  
377 in dry summers, leading to 3-5% increases in SOM stocks in a 30-year perspective. Table 5 suggests that tillage is  
378 one of the least sensitive factors affecting SOM stocks: doubling the tillage intensity parameter in the model,  $k_{ill}$ ,  
379 only reduces SOM stocks by 4 to 5%. It must be admitted, however, that the simple description of tillage effects  
380 in the model is yet to be rigorously and systematically tested. Nevertheless, in a meta-analysis of long-term  
381 experiments in boreal/temperate climates, Haddaway et al. (2017) and Meurer et al. (2018) only found larger SOC  
382 stocks under no-till compared with conventional tillage in the topsoil, while no overall significant effect of tillage  
383 system on SOC stocks was detected for soil profiles to 60 cm depth.



384  
385 **Figure 7. Distributions of mean residence times for SOM calculated in the sensitivity analysis for four depths**  
386 **in the soil profiles of production area PO4 in east-central Sweden. Horizontal lines show median values, the**  
387 **box defines the inter-quartile range, error bars define 10<sup>th</sup> and 90<sup>th</sup> percentiles and solid symbols indicate**  
388 **5<sup>th</sup> and 95<sup>th</sup> percentiles.**

389





390 **Table 5. Parameter sensitivity (NRC = normalized regression coefficients)**

Parameter	NRC	
$k_o$	Decomposition rate constant (old OM)	-0.833
$F_p$	Physical protection factor	-0.695
$A_a$	Microbial energy limitation factor	0.606
$HI$	Harvest index	-0.513
$Y$	Crop Yield	0.401
$\epsilon$	OM retention coefficient	0.329
$f_{bg}$	Fraction of NPP allocated below-ground	0.291
$k_y$	Decomposition rate constant (young OM)	-0.174
$f_{clay}$	Clay content	0.128
$f_{inc}$	Fraction of above-ground residues incorporated	0.127
$k_{till}$	Tillage transfer coefficient	-0.045
$w_s$	Factor for soil strength effects on root distribution	0.035
$D_{95}$	Root depth	-0.023
$\psi_{mic}$	Pressure head defining micropore region	-0.015
$c$	Root depth distribution factor	-0.009

391 **4 Concluding remarks**

392 We presented here a novel parsimonious or “minimalist” model that simulates the emergent effects of soil texture  
 393 and soil structure on C stocks and turnover rates in soil profiles by mimicking two of the key processes involved  
 394 in C stabilization (i.e. physical protection and microbial energy limitation). Parameters controlling these processes  
 395 were also found to be among the most sensitive in the model. However, the decomposition rate constant for old  
 396 microbial-processed OM,  $k_o$  was the most sensitive parameter in the model. Although  $k_o$  should be considered as  
 397 a lumped parameter reflecting the influence of various processes, the available experimental evidence suggests  
 398 that the strength of adsorption and OM-mineral interactions controlling the bioavailability of the substrate (i.e.  
 399 chemical protection) should be the most important factor underlying its variation (e.g. Lehmann and Kleber, 2015;  
 400 Mathieu et al., 2015; Doetterl et al., 2015). The development of pedotransfer approaches (van Looy et al., 2017)  
 401 to estimate  $k_o$  using soil properties such as clay content and clay mineralogy, pH and Al and Fe oxides (e.g. Mathieu  
 402 et al., 2015; Rasmussen et al., 2018; Fukumasu et al., 2021) would therefore be helpful in supporting predictive  
 403 model applications at larger scales.

404 The comparisons of model predictions with local- and regional-scale data confirm that it shows promise. Despite  
 405 equifinality, the parameters regulating decomposition in the model could be identified within reasonably narrow  
 406 ranges using data from a long-term field experiment with three treatments characterized by strongly contrasting  
 407 OM inputs for more than 50 years. Ideally, the model should now be further tested at multiple sites using data from  
 408 long-term field experiments, including comparisons of alternative cropping systems and tillage management (i.e.  
 409 no-till vs. conventional systems).



410 **Competing interests**

411 The contact author has declared that none of the authors has any competing interests.

412 **References**

- 413 Ahrens, B., Braakhekke, M., Guggenberger, G., Schrumpf, M., Reichstein, M. 2015. Contribution of sorption,  
414 DOC transport and microbial interactions to the  $^{14}\text{C}$  age of a soil organic carbon profile: Insights from a  
415 calibrated process model. *Soil Biology and Biochemistry*, 88, 390-402.
- 416 Balesdent, J., Mariotti, A. 1987. Natural  $^{13}\text{C}$  abundance as a tracer for studies of soil organic matter dynamics. *Soil*  
417 *Biology and Biochemistry*, 19, 25-30. [https://doi.org/10.1016/0038-0717\(87\)90120-9](https://doi.org/10.1016/0038-0717(87)90120-9)
- 418 Batjes, N. 1996. Total carbon and nitrogen in the soils of the world. *European Journal of Soil Science*, 47, 151-  
419 163.
- 420 Beven, K. 2006. A manifesto for the equifinality thesis. *Journal of Hydrology*, 320, 18-36.
- 421 Beven, K., Binley, A. 2014. GLUE: 20 years on. *Hydrological Processes*, 28, 5897-5918.
- 422 Bolinder, M., Janzen, H., Gregorich, E., Angers, D., VandenBygaart, A. 2007. An approach for estimating net  
423 primary productivity and annual carbon inputs to soil for common agricultural crops in Canada. *Agriculture,*  
424 *Ecosystems and Environment*, 118, 29-42.
- 425 Braakhekke, M., Beer, C., Hoosbeek, M., Reichstein, M., Kruijt, B., Schrumpf, M., Kabat, P. 2011. SOMPROF:  
426 A vertically explicit soil organic matter model. *Ecological Modelling*, 222, 1712-1730.
- 427 Braakhekke, M., Wutzler, T., Beer, C., Kattge, J., Schrumpf, M., Ahrens, B., Schoning, I., Hoosbeek, M., Kruijt,  
428 B., Kabat, P., Reichstein, M. 2013. Modeling the vertical soil organic matter profile using Bayesian  
429 parameter estimation. *Biogeosciences*, 10, 399–420.
- 430 Braakhekke, M., Beer, C., Schrumpf, M., Ekici, A., Ahrens, B., Hoosbeek, M., Kruijt, B., Kabat, P., Reichstein,  
431 M. 2014. The use of radiocarbon to constrain current and future soil organic matter turnover and transport  
432 in a temperate forest. *Journal of Geophysical Research: Biogeosciences*, 119, 372–391.
- 433 Brooks, R., Corey, A. 1964. Hydraulic properties of porous media. *Hydrology Paper 3*, Colorado State University,  
434 27 pp.
- 435 Button, E., Pett-Ridge, J., Murphy, D., Kuzyakov, Y., Chadwick, D., Jones, D. 2022. Deep-C storage: Biological,  
436 chemical and physical strategies to enhance carbon stocks in agricultural subsoils. *Soil Biology and*  
437 *Biochemistry*, 170, 108697.
- 438 Camino-Serrano, M., Guenet, B., Luysaert, S., Ciais, P., Bastrikov, V., De Vos, B., Gielen, B., Gleixner, G.,  
439 Jornet-Puig, A., Kaiser, K., Kothawala, D., Lauerwald, R., Peñuelas, J., Schrumpf, M., Vicca, S., Vuichard,  
440 N., Walmsley, D., Janssens, I. 2018. ORCHIDEE-SOM: modeling soil organic carbon (SOC) and dissolved  
441 organic carbon (DOC) dynamics along vertical soil profiles in Europe. *Geoscientific Model Development*,  
442 11, 937-957.
- 443 Chen, S., Zou, J., Hu, Z., Lu, Y. 2020. Temporal and spatial variations in the mean residence time of soil organic  
444 carbon and their relationship with climatic, soil and vegetation drivers. *Global and Planetary Change*, 195,  
445 103359.
- 446 Coucheney, E., Kätterer, T., Meurer, K.H.E., Jarvis, N. 2024. Improving the sustainability of arable cropping  
447 systems by modifying root traits: a modelling study for winter wheat. *European Journal of Soil Science*,  
448 75, e13524.



- 449 Derrien, D., Barré, P., Basile-Doelsch, I., Cécillon, L., Chabbi, A., Crème, A., Fontaine, S., Henneron, L., Janot,  
450 N., Lashermes, G., Quénéa, K., Rees, F., Dignac, M-F. 2013. Current controversies on mechanisms  
451 controlling soil carbon storage: implications for interactions with practitioners and policy-makers. A  
452 review. *Agronomy for Sustainable Development*, 43:21.
- 453 Doetterl, S., Stevens, A., Six, J., Merckx, R., Van Oost, K., Casanova Pinto, M., Casanova-Katny, A., Muñoz, C.,  
454 Boudin, M., Zagal Venegas, E., Boeckx, P. 2015. Soil carbon storage controlled by interactions between  
455 geochemistry and climate. *Nature Geoscience*, 8, DOI 10.1038/NGEO2516.
- 456 Eriksson, J., Matsson, L., Söderström, M. 2010. Current status of Swedish arable soils and cereal crops. Data from  
457 the period 2001-200 (in Swedish, with English summary). Report 6349, Swedish Environmental Protection  
458 Agency, Stockholm, 129 pp.
- 459 Fan, J., McConkey, B., Wang, H., Janzen, H. 2016. Root distribution by depth for temperate agricultural crops.  
460 *Field Crops Research*, 189, 68-74.
- 461 Fukumasu, J., Poelplau, C. Coucheney, E., Jarvis, N., Klöffel, T., Koestel, J., Kätterer, T., Nimblad Svensson, D.,  
462 Wetterlind, J., Larsbo, M. 2021. Oxalate-extractable aluminum alongside carbon inputs may be a major  
463 determinant for organic carbon content in agricultural topsoils in humid continental climate. *Geoderma*,  
464 402, 115345.
- 465 Garsia, A., Moinet, A., Vazquez, C., Creamer, R., Moinet, G. 2023. The challenge of selecting an appropriate soil  
466 organic carbon simulation model: A comprehensive global review and validation assessment. *Global  
467 Change Biology*, 29, 5760–5774.
- 468 Haddaway, N., Hedlund, K., Jackson, L., Kätterer, T., Lugato, E., Thomsen, I., Jørgensen, H., Isberg, P-E., 2017.  
469 How does tillage intensity affect soil organic carbon? A systematic review. *Environmental Evidence*, 6:30  
470 DOI 10.1186/s13750-017-0108-9.
- 471 Hay, R. 1995. Harvest index – a review of its use in plant-breeding and crop physiology. *Annals of Applied  
472 Biology*, 126, 197-216.
- 473 Hicks Pries, C., Sulman, B., West, C., O'Neill, C., Poppleton, E., Porras, R., Castanha, C., Zhui, B., Wiedemeier,  
474 D., Torn, M. 2018. Root litter decomposition slows with soil depth. *Soil Biology and Biochemistry*, 125,  
475 103-114.
- 476 Izaurralde, R., J.R. Williams, J., McGill, W., Rosenberg, N., Quiroga Jakas, M. 2006. Simulating soil C dynamics  
477 with EPIC: Model description and testing against long-term data. *Ecological Modelling*, 192, 362-384.
- 478 Jarvis, N., Coucheney, E., Lewan, E., Klöffel, T., Meurer, K., Keller, T., Larsbo, M. 2024. A new soil-crop model  
479 accounting for interactions between soil structure dynamics, hydrological processes and organic matter  
480 cycling. *European Journal of Soil Science*, 75, e13455.
- 481 Jenkinson, D., Coleman, K. 2008. The turnover of organic carbon in subsoils. Part 2. *European Journal of Soil  
482 Science*, 59, 400-413.
- 483 Jobbágy, E., Jackson, R. 2000. The vertical distribution of soil organic carbon and its relation to climate and  
484 vegetation. *Ecological Applications*, 10, 423–436.
- 485 Juston, J., Andrén, O., Kätterer, T., Jansson, P-E. 2010. Uncertainty analyses for calibrating a soil carbon balance  
486 model to agricultural field trial data in Sweden and Kenya. *Ecological Modelling*, 221, 1880-1888.



- 487 Kätterer, T., Andrén, O., Jansson, P-E. 2006. Pedotransfer functions for estimating plant available water and bulk  
488 density in Swedish agricultural soils. *Acta Agriculturae Scandinavica Section B – Soil and Plant Science*,  
489 56, 263-276.
- 490 Kätterer, T., Bolinder, M., Andrén, O., Kirchmann, H., Menichetti, L. 2011. Roots contribute more to refractory  
491 soil organic matter than above-ground crop residues, as revealed by a long-term field experiment.  
492 *Agriculture, Ecosystems and Environment*, 141, 184-192.
- 493 Keyvanshokouhi, S., Cornu, S., Lafolie, F., Balesdent, J., Guenet, B., Moitrier, N., Moitrier, N., Nougier, C., Finke,  
494 P. 2019. Effects of soil process formalisms and forcing factors on simulated organic carbon depth-  
495 distributions in soils. *Science of the Total Environment*, 652, 523-537.
- 496 Klöffel, T., Barron, J., Nemes, A., Giménez, D., Jarvis, N. 2024. Soil, climate, time and site factors as drivers of  
497 soil structure evolution in agricultural soils from a temperate-boreal region. *Geoderma*, 442, 116772.
- 498 Kravchenko, A., Negassa, W., Guber, A., Rivers, M. 2015. Protection of soil carbon within macro-aggregates  
499 depends on intra-aggregate pore characteristics. *Scientific Reports*, 5, 16261 DO: 10.1038/srep 16261.
- 500 Lehmann, J., Kleber, M. 2015. The contentious nature of soil organic matter. *Nature*, 528,  
501 doi:10.1038/nature16069
- 502 Le Noë, J., Manzoni, S., Abramoff, R., Bölscher, T., Bruni, E., Cardinael, R., Ciais, P., Chenu, C., Clivot, H.,  
503 Derrien, D., Ferchaud, F., Garnier, P., Goll, D., Lashermes, G., Martin, M., Rasse, D., Rees, F., Sainte-  
504 Marie, J., Salmon, E., Schiedung, M., Schimel, J., Wieder, W., Abiven, S., Barré, P., Cécillon, L., Guenet,  
505 B. 2013. Soil organic carbon models need independent time-series validation for reliable prediction.  
506 *Communications Earth and Environment*, 4:158, <https://doi.org/10.1038/s43247-023-00830-5>.
- 507 Mathieu, J., Hatté, C., Balesdent, J., Parent, E. 2015. Deep soil carbon dynamics are driven more by soil type than  
508 by climate: a worldwide meta-analysis of radiocarbon profiles. *Global Change Biology*, 21, 4278-4292.
- 509 Meurer, K., Haddaway, N., Bolinder, M., Kätterer, T., 2018. Tillage intensity affects total SOC stocks in boreo-  
510 temperate regions only in the topsoil – A systematic review using an ESM approach. *Earth-Science*  
511 *Reviews*, 177, 613-622.
- 512 Meurer, K., Chenu, C., Coucheney, E., Herrmann, A., Keller, T., Kätterer, T., Nimblad Svensson, D., Jarvis, N.  
513 2020. Modelling dynamic interactions between soil structure and the storage and turnover of soil organic  
514 matter. *Biogeosciences*, 17, 5025-5042.
- 515 Paustian, K., Lehmann, J., Ogle, S., Reay, D., Robertson, G., Smith, P. 2016. Climate-smart soils. *Nature*,  
516 532(7597), 49-57.
- 517 Persson, J., Kirchmann, H. 1994. Carbon and nitrogen in arable soils as affected by supply of N fertilizers and  
518 organic manures. *Agriculture, Ecosystems and Environment*, 51, 249-255.
- 519 Poeplau, C., Don, A., Schneider, F. 2021. Roots are key to increasing the mean residence time of organic carbon  
520 entering temperate agricultural soils. *Global Change Biology*, 27, 4921–4934.
- 521 Rasmussen, C., Heckman, K., Wieder, W., Keiluweit, M., Lawrence, C., Berhe, A., Blankinship, J., Crow, S.,  
522 Druhan, J., Hicks Pries, C., Marin-Spiotta, E., Plante, A., Schädel, C., Schimel, J., Sierra, C., Thompson,  
523 A., Wagai, R. 2018. Beyond clay: towards an improved set of variables for predicting soil organic matter  
524 content. *Biogeochemistry*, 137, 297-306.
- 525 Rasse, D., Rumpel, C., Dignac, M. 2005. Is soil carbon mostly root carbon? Mechanisms for a specific stabilisation.  
526 *Plant and Soil*, 269, 341-356.



- 527 Riley, W., Maggi, F., Kleber, M., Torn, M., Tang, J., Dwivedi, D., Guerry, N. 2014. Long residence times of  
528 rapidly decomposable soil organic matter: application of a multi-phase, multi-component, and vertically  
529 resolved model (BAMS1) to soil carbon dynamics. *Geoscientific Model Development*, 7, 1335–1355.
- 530 Ruamps, L., Nunan, N., Chenu, C. 2011. Microbial biogeography at the soil pore scale. *Soil Biology and*  
531 *Biochemistry*, 43, 280-286.
- 532 Rumpel, C., Kögel-Knabner, I. 2011. Deep soil organic matter-a key but poorly understood component of  
533 terrestrial C cycle. *Plant and Soil*, 338, 143–158.
- 534 Salomé, C., Nunan, N., Pouteau, V., Lerch, T., Chenu, C. 2010. Carbon dynamics in topsoil and in subsoil may be  
535 controlled by different regulatory mechanisms. *Global Change Biology*, 16, 416-426.
- 536 Saltelli, A., Annoni, P. 2010. How to avoid a perfunctory sensitivity analysis. *Environmental Modelling and*  
537 *Software*, 25, 1508-1517.
- 538 Sanaullah, M., Chabbi, A., Leifeld, J., Bardoux, G., Billou, D., Rumpel, C. 2011. Decomposition and stabilization  
539 of root litter in top- and subsoil horizons: what is the difference? *Plant Soil* 338, 127–141.  
540 <https://doi.org/10.1007/s11104-010-0554-4>
- 541 Schenk, H.J., Jackson, R. 2002. The global biogeography of roots. *Ecological Monographs*, 72, 311-328.
- 542 Schiedung, H., Tilly, N., Hütt, C., Welp, G., Brüggemann, N., Amelung, W. 2017. Spatial controls of topsoil and  
543 subsoil organic carbon turnover under C3–C4 vegetation change. *Geoderma*, 303, 44-51.  
544 <https://doi.org/10.1016/j.geoderma.2017.05.006>
- 545 Sierra, C., Hoyt, A., He, Y., Trumbore, S. 2018. Soil organic matter persistence as a stochastic process: age and  
546 transit time distributions of carbon in soils. *Global Biogeochemical Cycles*, 32, 1574–1588.
- 547 Sierra, C., Ahrens, B., Bolinder, M., Braakhekke, M., von Fromm, S., Kätterer, T., Luo, Z., Parvin, N., Wang, G.  
548 2024. Carbon sequestration in the subsoil and the time required to stabilize carbon for climate change  
549 mitigation. *Global Change Biology*, 30:e17153.
- 550 Sleutel, S., De Neve, S., Beheydt, D., Li, C., Hofman, G. 2006. Regional simulation of long-term organic carbon  
551 stock changes in cropland soils using the DNDC model: 1. Large-scale model validation against a spatially  
552 explicit data set. *Soil Use and Management*, 22, 342-351.
- 553 Smerald, A., Rahimi, J., Scheer, C. 2023. A global dataset for the production and usage of cereal residues in the  
554 period 1997-2021. *Scientific Data*, 10, Article 685.
- 555 Smith, P., Lutfalla, S., Riley, W., Torn, M., Schmidt, M., Soussana, J-F. 2018. The changing faces of soil organic  
556 matter research. *European Journal of Soil Science*, 69, 23-30.
- 557 Van Looy K., Bouma J., Herbst M., Koestel J., Minasny B., Mishra U., Montzka C., Nemes A., Pachepsky Y.,  
558 Padarian J., Schaap M., Tóth B., Verhoef A., Vanderborght J., van der Ploeg M., Weihermüller L.,  
559 Zacharias S., Zhang Y., Vereecken H. 2017. Pedotransfer functions in Earth system science: challenges  
560 and perspectives. *Reviews of Geophysics*, doi: 10.1002/2017RG000581.
- 561 Wutzler, T., Reichstein, M. 2013. Priming and substrate quality interactions in soil organic matter models.  
562 *Biogeosciences*, 10, 2089-2103.
- 563 Yagasaki, Y., Shirato, Y. 2014. Assessment on the rates and potentials of soil organic carbon sequestration in  
564 agricultural lands in Japan using a process-based model and spatially explicit land-use change inventories  
565 – Part 1: Historical trend and validation based on nation-wide soil monitoring. *Biogeosciences*, 11, 4429-  
566 4442.



567 Yu, L., Ahrens, B., Wutzler, T., Marion Schruppf, M., Zaehle, S. 2020. Jena Soil Model (JSM v1.0; revision  
568 1934): a microbial soil organic carbon model integrated with nitrogen and phosphorus processes.  
569 Geoscientific Model Development, 13, 783–80

## 570 **5 Complementary information**

### 571 **Highlights**

- 572 • We outline a simple phenomenological model of soil organic carbon (SOC) turnover in a soil profile
- 573 • The model predicts effects of soil aggregation and microbial energy limitation on SOC persistence
- 574 • The model is tested using SOC data from treatments with varying C input in a long-term field trial
- 575 • The most influential parameters were identified in a sensitivity and uncertainty analysis

576 **Running title:** A simple model of SOC turnover in a soil profile

577 **Keywords:** aggregation, physical protection, microbial energy limitation, model, sensitivity

### 578 **Acknowledgments**

579 The work described in this paper was funded by the EU EJP SOIL project MaxRootC (“Optimizing roots for  
580 sustainable crop production in Europe – pure cultures and cover crops”) under the H2020 Grant agreement number  
581 862695 and by the Swedish Research Council for Sustainable Development (FORMAS, grant 2022-00214).  
582 Maintenance of the Ultuna Long-Term Field Experiment (RAM-56) is funded by the Faculty of Natural Resources  
583 and Agricultural Sciences at the Swedish University of Agricultural Sciences (SLU, Sweden). We would also like  
584 to thank Lorenzo Menichetti (formerly at SLU Department of Ecology, now at LUKE, The Natural Resources  
585 Institute of Finland) and Frédéric Rees (INRAE, France) for helpful discussions on this work.

### 586 **Authors email, ORCID-ID and contributions**

587 Email addresses and ORCID-ID in brackets:

588 [elsa.coucheney@slu.se](mailto:elsa.coucheney@slu.se) (0000-0001-5988-2085)

589 [anke.herrmann@slu.se](mailto:anke.herrmann@slu.se) (0000-0002-6273-1234)

590 [nicholas.jarvis@slu.se](mailto:nicholas.jarvis@slu.se) (0000-0001-6725-6762)

### 591 **AUTHOR CONTRIBUTIONS**

592 **ELSA COUCHENEY:** Conceptualization; methodology; writing – original draft; writing - review and editing.

593 **ANKE HERRMANN:** Investigation; data curation; funding acquisition; writing - review and editing.

594 **NICHOLAS JARVIS:** Conceptualization; formal analysis; funding acquisition; methodology; project  
595 administration; writing – original draft; writing - review and editing.